magnetic pressure (due to a fountainlike current feature with a vortex at the anode tip) could produce the observed cathode-directed motion of the plasma.

ACKNOWLEDGMENT

The authors wish to thank Dr. D. F. Düchs for his helpful criticisms.

*Research supported in part by the National Aeronautics and Space Administration under Grant No. NGR-09-005-025.

†Present address: Naval Research Laboratory, Washington, D. C. 20390.

[1]G. Fritz, R. W. Kreplin, J. F. Meekins, A. E. Unzicker, and H. Friedman, Astrophys. J. 148, L133 (1967); see also J. F. Meekins, R. W. Kreplin, T. A. Chubb, and H. Friedman, Science 162, 891 (1968).

[2]W. M. Neupert and M. Swartz, Astrophys. J. Letters 160, L189 (1970); see also W. M. Neupert, W. Gates, M. Swartz, and R. Young, Astrophys. J. 149, L79 (1967).

[3]L. Cohen, U. Feldman, M. Swartz, and J. H. Underwood, J. Opt. Soc. Am. 58, 843 (1968).

[4]L. L. House, Astrophys. J., Suppl. 18, 21 (1969).

[5]A. H. Gabriel and C. Jordan, Nature 221, 947 (1969).

[6]S. V. Lebedev, S. L. Mandel'shtam, and G. M. Rodin, Zh. Eksperim. i Teor. Fiz. 37, 349 (1959) [Soviet Phys. JETP 37, 248 (1960)].

[7]S. K. Händel, Arkiv Fysik 28, 303 (1964); also S. K. Händel and J. M. Berg, *ibid.* 31, 1 (1965).

[8]L. N. Khudyakova, E. K. Gutnikova, and L. V. Tarasova, Zh. Tekhn. Fiz. 34, 2044 (1964) [Soviet Phys. Tech. Phys. 9, 1572 (1965)].

[9]"Elkinit-3," manufactured by P. R. Mallory Mettalurgical Co., Indianapolis, Ind.

[10]V. E. Cosslett and W. C. Nixon, *X-Ray Microscopy* (Cambridge U. P., London, 1960), Chap. 3.

[11]B. Edlén and F. Tyrén, Nature 143, 940 (1939).

[12]B. Edlén, Physica 13, 545 (1947).

[13]N. V. Roth and R. C. Elton, Naval Research Laboratory Report No. NRL-6638, 1968 (unpublished).

[14]H. Flemberg, Arkiv Math. Astron. Fysik 28A, 1 (1942); see also Ref. 12, p. 553.

[15]N. J. Peacock, R. J. Speer, and M. G. Hobby, J. Phys. B. 2, 798 (1969).

[16]G. A. Sawyer, J. Quant. Spectry. Radiative Transfer 2, 467 (1962).

[17]R. D. Cowan (private communication).

[18]H. R. Griem, Astrophys. J. 156, L103 (1969); 161, L155 (1970).

[19]H. M. Epstein, W. J. Gallagher, P. J. Mallozzi, and T. F. Stratton, Phys. Rev. A 2, 146 (1970).

[20]R. C. Elton, Naval Research Laboratory Report No. 6738, 1968 (unpublished).

[21]R. C. Elton, in *Methods of Experimental Physics-Plasma Physics*, edited by H. R. Griem and R. H. Lovberg (Academic, New York, 1970), Chap. 4.

[22]C. M. Dozier, J. V. Gilfrich, and L. S. Birks, Appl. Opt. 6, 2136 (1967).

[23]That this assumption is reasonable is seen from the large increase in ionization potential along the isoelectronic sequence between lithiumlike and heliumlike ions. Therefore, the heliumlike and hydrogenic ion populations will dominate when they exist. The strong dependence on effective charge Z (Z^2 for bremsstrahlung and Z^4 for radiative recombination) of the continuum radiation further favors these ions.

[24]S. V. Lebedev, Zh. Tekhn. Fiz. 38, 171 (1968) [Soviet Phys. Tech. Phys. 13, 119 (1968)].

[25]K. V. Roberts and D. E. Potter, *Methods in Computational Physics*, edited by B. Alder, S. Fernbach, and M. Rotenberg (Academic, New York, 1970).

PHYSICAL REVIEW A VOLUME 3, NUMBER 3 MARCH 1971

Muonium. II. Observation of the Muonium Hyperfine-Structure Interval*

J. M. Bailey,† W. E. Cleland,‡ V. W. Hughes, R. Prepost,§ and K. Ziock‖

Gibbs Laboratory, Yale University, New Haven, Connecticut 06520

(Received 1 July 1970)

A full discussion is given of the microwave-spectroscopy resonance method of measuring the hyperfine-structure interval $\Delta\nu$ of the ground state of muonium, including the theoretical value for $\Delta\nu$, the transition frequencies, and the resonance line shape. A complete description is also given of our experimental method of measuring $\Delta\nu$ at strong magnetic field. The initial experimental results gave $\Delta\nu = 4461.3 \pm 2.0$ MHz, in good agreement with the theoretical value $\Delta\nu = 4463.282 \pm 0.062$ MHz. The first observations of muonium chemistry are described.

I. INTRODUCTION

The discovery[1,2] that muonium is formed when muons are stopped in argon gas and the rough measurement of its ground-state hyperfine-structure interval $\Delta\nu$ with the use of a static magnetic field[2,3] indicated that $\Delta\nu$ could be measured in a precision microwave resonance experiment. The principles of the experiment are to form polarized muonium by stopping polarized muons in a gas, to induce with microwave power a resonance transition between two unequally populated hfs magnetic substates which will result in a change in muon spin direction, and to observe this transition through

the resulting change in the decay positron angular distribution. The ultimate precision which can be attained in a measurement of $\Delta\nu$ can be expected to be a small fraction of the natural linewidth of the resonance line; since the natural linewidth will be $\gamma/\pi = 0.14$ MHz, where γ is the muon decay rate, and since $\Delta\nu$ is approximately 4500 MHz, a precision of 1 ppm or better for $\Delta\nu$ is a conceivable goal.

The principal interest in a precise measurement of $\Delta\nu$ is to provide a critical test of the electromagnetic properties of the muon, and, in particular, of the muon-electron interaction. Under the assumption that the muon is a Dirac particle with a mass 207 times the electron mass and with the standard coupling to the electromagnetic field, the theoretical value for $\Delta\nu$ can be calculated with high accuracy from the quantum-electrodynamic bound-state two-body equation.[4] Any breakdown of this basic assumption, such as the existence of an unknown coupling to the muon or electron fields,[5] would alter the theoretical value of $\Delta\nu$.

The present paper, Muonium II, is the second paper of a series on muonium and deals with the measurement of the hfs interval $\Delta\nu$ of muonium. Section II of this paper gives a detailed discussion of the theory of the experiment, including the theoretical value for $\Delta\nu$, the transition frequencies, and the theoretical resonance line shape. Section III discusses the experimental method and apparatus, Sec. IV gives the data and data analysis, and Sec. V gives the results on the initial observation of a resonance transition at strong magnetic field. A brief report of a portion of the research has been published.[6,7]

The third paper of this series will give a detailed discussion of our precision measurement of $\Delta\nu$ at strong magnetic field.[8] Recently an additional precision measurement of $\Delta\nu$ at strong magnetic field has been reported.[9] The precision measurement of $\Delta\nu$ at weak magnetic field[10,11] will also be discussed in the fourth paper of this series.

II. THEORY OF EXPERIMENT

A. Theoretical Value for $\Delta\nu$

Under the assumption that both the muon and the electron are Dirac particles with the conventional coupling to the electromagnetic field, the hfs interval $\Delta\nu$ of the ground state of muonium can be calculated with modern quantum-electrodynamic theory from the Bethe-Salpeter equation.[4,12] The result is expressed[13] as a series expansion in the small parameters α and m_e/m_μ

$$\Delta\nu_{\text{theor}} = [\tfrac{16}{3}\alpha^2 cR_\infty(\mu_\mu/\mu_B^e)][1+(m_e/m_\mu)]^{-3} \times (1+\tfrac{3}{2}\alpha^2 + a_e + \epsilon_1 + \epsilon_2 + \epsilon_3 - \delta_\mu), \quad (2.1)$$

in which

$$a_e = \frac{\alpha}{2\pi} - 0.3285\frac{\alpha^2}{\pi^2} + (0.55\pm ?)\frac{\alpha^3}{\pi^3},$$

$$\epsilon_1 = \alpha^2(\ln 2 - \tfrac{5}{2}), \qquad \epsilon_2 = -\frac{8\alpha^3}{3\pi}\ln\alpha(\ln\alpha - \ln 4 + \tfrac{281}{480}),$$

$$\epsilon_3 = \frac{\alpha^3}{\pi}(18.4\pm 5), \quad \delta_\mu = \frac{3\alpha}{\pi}\frac{m_e m_\mu}{m_\mu^2 - m_e^2}\ln\frac{m_\mu}{m_e},$$

where α is the fine structure constant, c is the velocity of light, R_∞ is the Rydberg constant, μ_μ is the muon magnetic moment, μ_B^e is the electron Bohr magneton $= e\hbar/2m_e c$, m_e is the electron mass, and m_μ is the muon mass.

The first bracketed factor is the Fermi value[14] for $\Delta\nu$, and the second bracketed factor is a reduced mass correction.[15] The third bracketed factor includes relativistic, radiative, and recoil contributions that are of higher order in the parameters α and m_e/m_μ. The term $\frac{3}{2}\alpha^2$ is a relativistic correction to the Fermi value.[16] The term a_e is the anomalous magnetic moment of the electron.[17-22] The terms ϵ_1, ϵ_2, and ϵ_3 are radiative correction terms,[13,23-26] and the term ϵ_3 has only been calculated approximately.[13] The term δ_μ is a relativistic recoil correction.[27,28] No higher-order terms in α or m_e/m_μ have been calculated.

The term μ_μ in the Fermi factor could alternatively have been written as[22]

$$\mu_\mu = \mu_B^\mu[1 + (\alpha/2\pi) + 0.76578(\alpha^2/\pi^2) + (21.4\pm 1.1)(\alpha^3/\pi^3) + (6.5\pm 0.5)\times 10^{-8}], \quad (2.2)$$

where μ_B^μ is the muon Bohr magneton $= e\hbar/2m_\mu c$. All the terms in the bracket are of pure quantum-electrodynamic origin except for the term 6.5×10^{-8} which is the hadron contribution to the muon magnetic moment. If the muon mass were known from direct measurement with sufficient accuracy, then μ_μ could be replaced in Eq. (2.1) by Eq. (2.2); however, m_μ is not known[5] as well as μ_μ, and hence it is more useful to express $\Delta\nu$ as in Eq. (2.1).

For evaluation of $\Delta\nu_{\text{theor}}$ from Eq. (2.1) it is useful to express the quantity μ_μ/μ_B^e as

$$\mu_\mu/\mu_B^e = (\mu_\mu/\mu_p)(\mu_p/\mu_e)(1+a_e), \quad (2.3)$$

where μ_p and μ_e are the proton and electron magnetic moments, respectively. The most accurate value for μ_μ/μ_p is obtained from the measurement of the ratio of the precession frequency of positive muons stopped in water f_μ to the NMR frequency of protons in the water sample f_p. This measured ratio is[29,30]

$$f_\mu/f_p = 3.183\,362 \pm 0.000\,030 \quad [9.4 \text{ ppm, as 1 standard deviation}]. \quad (2.4)$$

If the magnetic field seen by the muons in the water is the same as the magnetic field seen by the protons in the water, then μ_μ/μ_p will equal f_μ/f_p.

However, the magnetic shielding that the muons experience in water depends on the chemistry of muons in water during the short period of the muon mean life. This subject is not well enough understood[7] for us to be sure that the magnetic shielding for a muon equals that for a proton. Indeed a plausible model for muon chemistry in water predicts[31] that the magnetic shielding for a muon in water is less than that for a proton by about 16 ppm, so that

$$\mu_\mu/\mu_p = (f_\mu/f_p)(1 - 16\times10^{-6}) = 3.183\,311. \quad (2.5)$$

Because of the uncertainty about magnetic shielding, we choose the value

$$\mu_\mu/\mu_p = 3.183\,337 \pm 0.000\,041\ (13\ \text{ppm}). \quad (2.6)$$

This value is the mean of the values given in Eqs. (2.4)–(2.5), and the error is obtained by combining in quadrature the error of 9.4 ppm given in Eq. (2.4) and the value 8 ppm which is $\frac{1}{2}$ of the magnetic shielding difference for muons and protons predicted in the model mentioned above.

The other fundamental constants appearing in Eqs. (2.1) and (2.3) are taken to have the following values[32,33]:

$$\begin{aligned} c &= (2.997\,925\,0 \pm 0.000\,001\,0)\times10^{10}\ \text{cm/sec} \quad (0.3\ \text{ppm}),\\ R_\infty &= (1.097\,373\,12 \pm 0.000\,000\,11)\times10^{5}\ \text{cm}^{-1} \quad (0.1\ \text{ppm}),\\ \mu_p/\mu_e &= 0.001\,519\,270\,83 \pm 0.000\,000\,000\,46 \quad (0.3\ \text{ppm}),\\ \alpha^{-1} &= 137.036\,08 \pm 0.000\,26 \quad (1.9\ \text{ppm}),\\ m_\mu/m_e &= 206.768\,8 \pm 0.002\,7 \quad (13\ \text{ppm}). \end{aligned} \quad (2.7)$$

The value for α^{-1} is based principally on the measurement of e/h by the ac Josephson effect.[34–36] The value for m_μ/m_e is obtained from the relation

$$m_\mu/m_e = (\mu_p/\mu_\mu)(\mu_e/\mu_p)\left|g_\mu/g_e\right|, \quad (2.8)$$

in which g_e and g_μ are the electron and muon g values, respectively. In addition to the values for μ_μ/μ_p and μ_e/μ_p given in Eqs. (2.6) and (2.7), the following experimental values for g_μ[37] and g_e[38] are used:

$$\begin{aligned} g_\mu &= -2(1.001\,166\,16 \pm 0.000\,000\,31) \quad (0.31\ \text{ppm}),\\ g_e &= 2(1.001\,159\,644 \pm 0.000\,000\,007) \quad (0.03\ \text{ppm}). \end{aligned} \quad (2.9)$$

Using Eq. (2.1) and the values for the constants given in Eqs. (2.6) and (2.7), we obtain

$$\Delta\nu_{\text{theor}} = \alpha^2(\mu_\mu/\mu_p)(2.632\,944\times10^7 \pm 2\ \text{ppm})\,\text{MHz}, \quad (2.10a)$$

$$\Delta\nu_{\text{theor}} = 4463.282 \pm 0.062\ \text{MHz} \quad (14\ \text{ppm}). \quad (2.10b)$$

The uncertainty in $\Delta\nu_{\text{theor}}$ is due almost entirely to the uncertainty in μ_μ/μ_p.

Various speculations have been made about unknown interactions which could alter the theoretical value for $\Delta\nu$ given in Eq. (2.10) which is based on conventional modern quantum electrodynamics. Since the theoretical formula for $\Delta\nu$ includes the values of the electron and muon magnetic moments or g values, any breakdown in the theories of these g values will alter the theoretical value of $\Delta\nu$. Possible causes of a breakdown have been discussed extensively either in terms of a modification of lepton or photon propagators or of vertex functions, or in terms of new field and couplings.[5,22,39–46] These new couplings include couplings to a "heavy photon," to the intermediate vector boson W, to neutral hadronic bosons, and to "heavy electrons." In addition, the muon-electron coupling,[5,39,47] and hence the value of $\Delta\nu$, would be changed by a change in the photon propagator such as that due to a heavy photon,[42] by a scalar coupling,[48] or by the existence of a neutral lepton current such as that associated with a direct coupling of muonium to antimuonium[5,49] ($\mu^+e^- \to \mu^-e^+$). Furthermore, the theoretical value of $\Delta\nu$ involves the relativistic quantum-electrodynamic bound-state equation, and any modification of this equation or of its use, such as the approximation of a many-time formalism by a single-time treatment, will alter $\Delta\nu$.[43,50]

B. Transition Frequencies

The relevant part of the Hamiltonian for the ground state of muonium in an external static magnetic field, and the associated energy eigenvalues and eigenfunctions have been discussed.[2,51] The Hamiltonian is

$$\mathcal{H} = a\vec{I}_\mu\cdot\vec{J} + \mu_B^e g_J\vec{J}\cdot\vec{H} + \mu_B^\mu g'_\mu\vec{I}_\mu\cdot\vec{H}\ . \quad (2.11)$$

The energy eigenvalues are

$$W_{F=1/2\pm1/2,M_F} = -\tfrac{1}{4}\Delta W + \mu_B^\mu g'_\mu M_F H \pm \tfrac{1}{2}\Delta W(1 + 2M_F x + x^2)^{1/2}\ , \quad (2.12)$$

in which $a = \Delta W$ is the hfs coupling constant, $\vec{I}_\mu$ is the muon spin operator, $\vec{J}$ is the electron angular momentum operator, g_J is electron gyromagnetic ratio in muonium, g'_μ is the muon gyromagnetic ratio in muonium, $\vec{H}$ is the external static magnetic field, $x = (g_J\mu_B^e - g'_\mu\mu_B^\mu)H/\Delta W$, F is the total angular momentum quantum number, and M_F is the associated magnetic quantum number. The quantities g_J and g'_μ are related to the free-electron and muon g values g_e and g_μ by the equations[52,53]

$$\begin{aligned} g_J &= g_e(1 - \tfrac{1}{3}\alpha^2) = 2(1.001\,141\,873 \pm 0.000\,000\,007)\ (0.03\ \text{ppm}),\\ g'_\mu &= g_\mu(1 - \tfrac{1}{3}\alpha^2) = -2(1.001\,148\,39 \pm 0.000\,000\,31)\ (0.31\ \text{ppm}). \end{aligned} \quad (2.13)$$

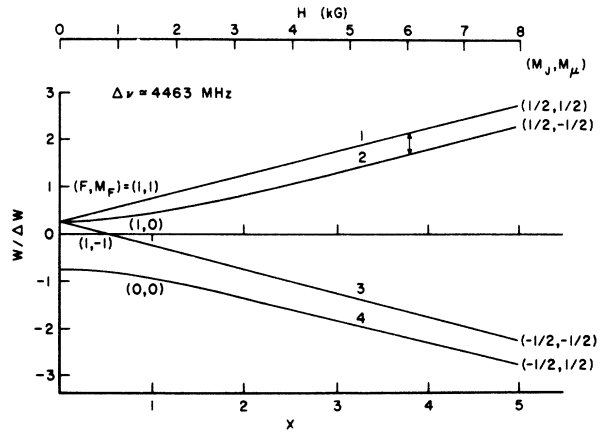

FIG. 1. Energy-level diagram for muonium in its $1^2S_{1/2}$ ground state in a magnetic field, as given by Eq. (2.12). At zero magnetic field, the energy difference between the $F=1$ and $F=0$ states is the hfs interval $\Delta W = h\Delta\nu$. The states are labeled 1–4 for convenience. The strong-field quantum numbers M_J (magnetic quantum number for z component of electronic angular momentum) and M_μ (magnetic quantum number for z component of muon spin) are shown for the levels. The transition indicated between states 1 and 2 is the one studied in this paper.

From Eqs. (2.7), (2.10), and (2.13) we find $x = H/1585$. The energy-level diagram corresponding to Eq. (2.12) is shown in Fig. 1 with the states labeled for convenience.

The four transition frequencies ν_{12}, ν_{14}, ν_{24}, and ν_{34} are of particular interest, as will be discussed in Sec. IIC; these frequencies are given below and are plotted in Fig. 2.

$$\nu_{12} = \frac{W_{1,1} - W_{1,0}}{h} = \frac{\mu_B^\mu g'_\mu H}{h} + \tfrac{1}{2}\Delta\nu\left[(1+x) - (1+x^2)^{1/2}\right],$$

$$\nu_{14} = \frac{W_{1,1} - W_{0,0}}{h} = \frac{\mu_B^\mu g'_\mu H}{h} + \tfrac{1}{2}\Delta\nu\left[(1+x) + (1+x^2)^{1/2}\right],$$

$$\nu_{24} = \frac{W_{1,0} - W_{0,0}}{h} = \Delta\nu\left[(1+x^2)^{1/2}\right], \tag{2.14}$$

$$\nu_{34} = \frac{W_{1,-1} - W_{0,0}}{h} = \frac{-\mu_B^\mu g'_\mu H}{h} + \tfrac{1}{2}\Delta\nu\left[(1-x) + (1+x^2)^{1/2}\right].$$

In the limit of strong magnetic field ($x \gg 1$) the transition frequencies of Eq. (2.14) are given approximately by the expressions

$$\nu_{12} = \tfrac{1}{2}\Delta\nu + \frac{\mu_B^\mu g'_\mu H}{h}, \qquad \nu_{14} = \tfrac{1}{2}\Delta\nu + \frac{\mu_B^e g_J H}{h},$$

$$\nu_{24} = \frac{\mu_B^e g_J H}{h} - \frac{\mu_B^\mu g'_\mu H}{h}, \qquad \nu_{34} = \tfrac{1}{2}\Delta\nu - \frac{\mu_B^\mu g'_\mu H}{h}. \tag{2.15}$$

In the limit of weak magnetic field ($x \ll 1$) the transition frequencies of Eqs. (2.14) are given approximately by the expressions

$$\nu_{12} = \frac{g_J \mu_B^e}{2h} + \frac{g'_\mu \mu_B^\mu H}{2h}, \qquad \nu_{14} = \Delta\nu + \frac{g_J \mu_B^e H}{2h} + \frac{g'_\mu \mu_B^\mu H}{2h},$$

$$\nu_{24} = \Delta\nu, \qquad \nu_{34} = \Delta\nu - \frac{g_J \mu_B^e H}{2h} - \frac{g'_\mu \mu_B^\mu H}{2h}. \tag{2.16}$$

It is useful to give expressions for the partial derivatives with respect to magnetic field H of the transition frequencies of Eqs. (2.14),

$$\frac{\partial\nu_{12}}{\partial H} = \frac{g_J \mu_B^e}{2h}\left(1 - \frac{x}{(1+x^2)^{1/2}}\right) + \frac{g'_\mu \mu_B^\mu}{2h}\left(1 + \frac{x}{(1+x^2)^{1/2}}\right),$$

$$\frac{\partial\nu_{14}}{\partial H} = \frac{g_J \mu_B^e}{2h}\left(1 + \frac{x}{(1+x^2)^{1/2}}\right) + \frac{g'_\mu \mu_B^\mu}{2h}\left(1 - \frac{x}{(1+x^2)^{1/2}}\right),$$

$$\frac{\partial\nu_{24}}{\partial H} = \left(\frac{g_J \mu_B^e - g'_\mu \mu_B^\mu}{h}\right)\left(\frac{x}{(1+x^2)^{1/2}}\right), \tag{2.17}$$

$$\frac{\partial\nu_{34}}{\partial H} = -\frac{g_J \mu_B^e}{2h}\left(1 - \frac{x}{(1+x^2)^{1/2}}\right) - \frac{g'_\mu \mu_B^\mu}{2h}\left(1 + \frac{x}{(1+x^2)^{1/2}}\right).$$

C. Theory of Resonance Line Shape

Transitions are induced between the hfs magnetic substates of muonium by application of a microwave magnetic field. The associated time-

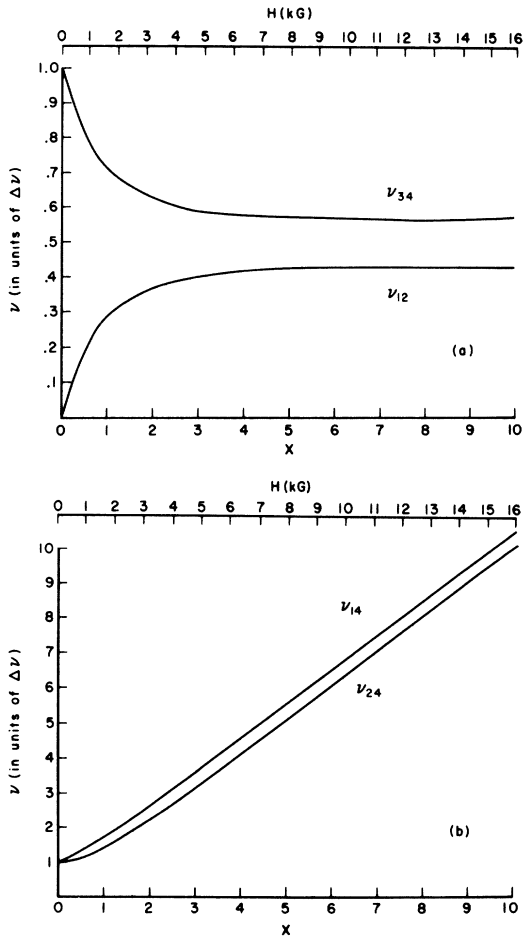

FIG. 2. (a) Plot of resonance frequencies ν_{12} and ν_{34} in units of $\Delta\nu$ versus x or H, as given in Eqs. (2.14). (b) Plot of resonance frequencies ν_{14} and ν_{24} in units of $\Delta\nu$ versus x or H, as given in Eqs. (2.14).

dependent Hamiltonian term is given by

$$\mathcal{H}' = (g_J \mu_B^e \vec{J} + g'_\mu \mu_B^\mu \vec{I}_\mu) \cdot \vec{H}_1 \cos\omega t = \mathcal{H}'_0 \cos\omega t , \quad (2.18)$$

in which $\vec{H}_1$ is the vector amplitude of the applied microwave field and ω is its angular frequency.

In the present treatment we shall make the following simplifying assumptions:

(a) Only two of the four muonium states need to be considered (designate them 1 and 2), since we are dealing with a resonance phenomenon and only the angular frequency difference ω_{12} will be approximately equal to the applied angular frequency ω. In the fourth paper of this series we will treat a more general three-state case.

(b) Time-dependent terms for the state amplitudes involving the nonresonant factors $e^{\pm i(\omega_{12}+\omega)t}$ are omitted. These terms produce a small modification to the resonance line shape[54] given in Eq. (2.28), and this modification is discussed in the third paper of this series.

(c) Muon decay into a positron and two neutrinos is treated phenomenologically in Eqs. (2.19) for the state amplitudes by the terms $\frac{1}{2}a\gamma$, in which a is a state amplitude and γ is the muon decay rate [$\gamma = 4.5490(17)\times 10^5$ sec^{-1}].[55] The justification for this type of phenomenological treatment of a decaying state has been discussed for the case in which the decay occurs due to the electromagnetic interaction.[56–58]

The time-dependent equations for the state amplitudes are then given by[51]

$$\dot{a}_1 = -ia_2 b e^{+i(\omega_{12}-\omega)t} - \tfrac{1}{2}a_1\gamma , \qquad \dot{a}_2 = -ia_1 b^* e^{-i(\omega_{12}-\omega)t} - \tfrac{1}{2}a_2\gamma , \quad (2.19)$$

in which the following notation has been used: The state function $\Psi(t)$ is expressed as

$$\Psi(t) = \phi(\vec{r})[a_1(t)\chi_1 e^{-iW_1 t/\hbar} + a_2(t)\chi_2 e^{-iW_2 t/\hbar}] ,$$

where $\phi(\vec{r})$ is the spatial part of the wave function, and χ_1 and χ_2 are spin eigenfunctions.[2] The subscripts 1 and 2 designate any two of the four hfs magnetic substates with corresponding energies W_1 and W_2, with $W_1 > W_2$. Furthermore,

$$\omega_{12} = (W_1 - W_2)/\hbar , \quad b = (\chi_1^* | \mathcal{H}'_0 | \chi_2)/(2\hbar) . \quad (2.19')$$

It is assumed that the diagonal matrix elements of $\mathcal{H}'_0$ in states 1 and 2 are zero.

Solution of Eqs. (2.19) yields

$$a_1(t) = \left\{ a_1(0) \left[\cos(\tfrac{1}{2}\Gamma t) - i\left(\frac{\omega_{12}-\omega}{\Gamma}\right)\sin(\tfrac{1}{2}\Gamma t)\right] + a_2(0)\left[-\frac{i2b}{\Gamma}\sin(\tfrac{1}{2}\Gamma t)\right]\right\} \times \exp\{-\tfrac{1}{2}\gamma t + [\tfrac{1}{2}i(\omega_{12}-\omega)]t\} ,$$

$$a_2(t) = \left[a_1(0)\left(-\frac{i2b^*}{\Gamma}\sin(\tfrac{1}{2}\Gamma t)\right) + a_2(0)\left(\cos(\tfrac{1}{2}\Gamma t) + \frac{i(\omega_{12}-\omega)}{\Gamma}\sin(\tfrac{1}{2}\Gamma t)\right)\right] \times \exp\{-\tfrac{1}{2}\gamma t + [\tfrac{1}{2}i(\omega_{12}-\omega)]t\} \quad (2.20)$$

in which $\Gamma = [(\omega-\omega_{12})^2 + 4|b|^2]^{1/2}$. The quantities $a_1(0)$ and $a_2(0)$ are the initial-state amplitudes at time $t = 0$.

A case of particular interest is that in which the initial conditions are

$$a_1(0) = 1, \quad a_2(0) = 0.$$

Hence

$$|a_1(t)|^2 = \left[\cos^2(\tfrac{1}{2}\Gamma t) + \left(\frac{\omega_{12}-\omega}{\Gamma}\right)^2 \sin^2(\tfrac{1}{2}\Gamma t)\right] e^{-\gamma t} , \quad (2.21)$$

$$|a_2(t)|^2 = \frac{4|b|^2}{\Gamma^2}\sin^2(\tfrac{1}{2}\Gamma t)e^{-\gamma t} .$$

The quantity $|a_2(t)|^2$ attains its maximum value for $t = 1/\gamma$ of $1/e$ at resonance ($\omega = \omega_{12}$) when $|b|t = \frac{1}{2}\pi$.

The matrix element b determines the selection rules and probabilities for transitions between states. Table I gives the value of b for all the pairs of states. The selection rules are the usual ones for a magnetic dipole transition:

$$\Delta F = 0, \pm 1 , \quad \Delta M_F = 0 \quad \text{for } \vec{H}_1 = H_z\hat{k} , \quad \Delta M_F = \pm 1 \quad \text{for } H_1 = H_x\hat{i} + H_y\hat{j} . \quad (2.22)$$

We do not observe the muonium-state populations directly. Rather the quantity observed as the resonance signal is the number of decay positrons emitted in a particular direction, which is one aspect of the angular distribution of the decay positrons. The decay of the muon in muonium is not significantly influenced by the electron in muonium, except insofar as the electron influences the spin state of the muon. Hence if we observe the number of positrons emitted in the z direction, the only relevant quantity which depends on the muonium state is the z component of the muon spin $\langle I_{\mu z}\rangle$. For the two-state case discussed, the z component of the muon polarization P_z is given by

$$P_z(t) = P_{z0}(t)e^{-\gamma t} = \langle \Psi^* | 2I_{\mu z} | \Psi \rangle = |a_1|^2(\chi_1^* | 2I_{\mu z} | \chi_1) + |a_2|^2(\chi_2^* | 2I_{\mu z} | \chi_2) + a_1^* a_2(\chi_1^* | 2I_{\mu z} | \chi_2)e^{i\omega_{12}t} + a_2^* a_1(\chi_2^* | 2I_{\mu z} | \chi_1)e^{i\omega_{12}t} . \quad (2.23)$$

The probability of emission of a decay positron with momentum y in the direction θ per unit time is given by[1,5,59,60]

TABLE I. Matrix elements of b for $\vec{H}_1 = H_x\hat{i} + H_y\hat{j} + H_z k$. The quantity b is defined by Eqs. (2.18) and (2.19′). The spin functions for the four states defined in Fig. 1 are given in Eq. (2.4) of Ref. 2. The quantities s and c are defined by $s = \sin(\frac{1}{2}\,\mathrm{arccot}\,x)$ and $c = \cos(\frac{1}{2}\,\mathrm{arccot}\,x)$. The quantity x is defined in Eq. (2.11). The quantities B_J and B_I are defined by $B_J = \frac{1}{4}(g_J\mu_B^e/\hbar)$ and $B_I = \frac{1}{4}(g_\mu'\mu_B^\mu/\hbar)$.

Final state \ Initial state	1	2	3	4
1	$(B_J + B_I)H_z$	$(sB_J + cB_I)(H_x - iH_y)$	0	$(cB_J - sB_I)(H_x - iH_y)$
2	$(sB_J + cB_I)(H_x + iH_y)$	$(c^2 - s^2)(B_J - B_I)H_z$	$(cB_J + sB_I)(H_x - iH_y)$	$-2sc(B_J - B_I)H_z$
3	0	$(cB_J + sB_I)(H_x + iH_y)$	$-(B_J + B_I)H_z$	$(-sB_J + cB_I)(H_x + iH_y)$
4	$(cB_J - sB_I)(H_x + iH_y)$	$-2sc(B_J - B_I)H_z$	$(-sB_J + cB_I)(H_x - iH_y)$	$(s^2 - c^2)(B_J - B_I)H_z$

$$N(y, \theta, t)\,dy\,d\Omega = (2\pi)^{-1}\gamma y^2[(3-2y) + (2y-1)P_{z0}(t)\cos\theta]e^{-\gamma t}\,dy\,d\Omega, \quad (2.24)$$

in which y is measured in the unit of $\frac{1}{2}m_\mu c$ and θ is the polar angle with respect to the z axis. Usually decay positrons of essentially all momenta are observed, so we consider

$$N(\theta, t)\,d\Omega = \int_0^1 N(y, \theta, t)\,dy\,d\Omega = (4\pi)^{-1}\gamma[1 + \tfrac{1}{3}P_{z0}(t)\cos\theta]e^{-\gamma t}\,d\Omega. \quad (2.25)$$

It is also approximately true that the observation of decay positrons occurs for all times $0 \le t \le \infty$. Hence we calculate

$$N(\theta) = \int_0^\infty N(\theta, t)\,dt$$

using Eqs. (2.23) and (2.25):

$$N(\theta) = \frac{d\Omega}{4\pi}\left(1 + \tfrac{1}{3}\gamma\cos\theta\left[(\chi_1^*|2I_{\mu z}|\chi_1)\int_0^\infty |a_1|^2\,dt + (\chi_2^*|2I_{\mu z}|\chi_2)\int_0^\infty |a_2|^2\,dt\right]\right). \quad (2.26)$$

We have assumed that the muon decay rate γ is very small compared to the resonance frequency ω_{12} which will be true for the transitions to be studied, and hence the small contribution from the cross-product terms in Eq. (2.23) which involve $a_1^* a_2$ and $a_2^* a_1$ are neglected in Eq. (2.26).

The special case given in Eq. (2.21) is of particular interest, and for this case Eq. (2.26) becomes

$$N(\theta) = \frac{d\Omega}{4\pi}\left\{1 + \tfrac{1}{3}\cos\theta\left[(\chi_1^*|2I_{\mu z}|\chi_1)\left(1 - \frac{2|b|^2}{\Gamma^2+\gamma^2}\right) + (\chi_2^*|2I_{\mu z}|\chi_2)\left(\frac{2|b|^2}{\Gamma^2+\gamma^2}\right)\right]\right\}. \quad (2.27)$$

The signal $\Delta N(\theta)$ in our resonance experiment is the difference between the number of positrons observed with the microwave magnetic field on and with the microwave magnetic field off, and when normalized for a single muon it is given by

$$\Delta N(\theta) = \frac{d\Omega\cos\theta}{12\pi}\left[-(\chi_1^*|2I_{\mu z}|\chi_1) + (\chi_2^*|2I_{\mu z}|\chi_2)\right]\frac{2|b|^2}{\Gamma^2+\gamma^2}. \quad (2.28)$$

This line shape of Eq. (2.28) is a Lorentzian line shape with regard to variation of the applied frequency ω, and it has its maximum value when $\omega = \omega_{12}$. The full width between the half-intensity points is given by

$$\Delta\omega_{1/2} = 2\pi\Delta f_{1/2} = 2(4|b|^2 + \gamma^2)^{1/2}. \quad (2.29)$$

In the limit of zero microwave power ($|b|^2 = 0$), we would obtain the natural linewidth

$$\Delta f_{1/2} = \gamma/\pi = 0.145\ \mathrm{MHz}. \quad (2.30)$$

A nonzero value of $|b|^2$ contributes power broadening of the line. At resonance, the signal intensity $\Delta N(\theta)_{\max}$ is proportional to

$$\Delta N(\theta)_{\max} \propto |b|^2/(4|b|^2 + \gamma^2). \quad (2.31)$$

III. EXPERIMENTAL METHOD AND APPARATUS

A. Introduction

The transition studied in the present paper and in the third paper of this series is that between states 1 and 2 at strong magnetic field H (see Fig. 1), whose frequency ν_{12} is given in Eqs. (2.14) and plotted in Fig. 2. This choice of transition was based on the following considerations:

(a) A transition between two states at strong magnetic field produces a larger signal than a transition at weak magnetic field because of the larger change in the polarization of the muons. It is necessary, of course, to choose an allowed transition for which $\Delta M_\mu = \pm 1$, and hence either transition $1 \leftrightarrow 2$ or $3 \leftrightarrow 4$ was needed, and indeed either could have been used. (See below for a further discussion of signal intensity.) It is apparent from Eqs. (2.15) that transition $2 \leftrightarrow 4$ is not useful since its frequency ν_{24} in the strong field case does not depend on $\Delta\nu$, which is the quantity to be measured.

(b) At strong static magnetic field, depolarization of the muons (in the absence of the microwave field) is expected to be small due to the strong coupling of the muon magnetic moment to the static magnetic field.

(c) The actual magnetic field value used of about

6000 G ($x \simeq 3.8$) was the maximum field attainable with the available magnets and power supplies.

A schematic diagram of the experimental arrangement[61] is shown in Fig. 3. Incident polarized muons produced by the Columbia University Nevis synchrocyclotron are stopped in a high-pressure pure-argon-gas target, which contains a microwave cavity. As discussed in a previous paper,[2] close to 100% of the stopped muons form muonium, and in the strong magnetic field H of 6000 G, the muonium-state populations formed will be approximately $p_1 = \frac{1}{2}$, $p_2 = 0$, $p_3 = 0$, and $p_4 = \frac{1}{2}$ [see Eq. (3.11), Ref. 2]. Decay positrons are counted by the telescope of counters 3 and 4. In the absence of microwave power, muons decay from the initially formed muonium-state populations and the decay positrons are emitted preferentially towards counter 2 [see Eqs. (2.9) of Ref. 2]. In the presence of microwave power at the resonance frequency ν_{12}, the probability that muonium is in state 2 is increased and the probability that it is in state 1 is decreased [see Eq. (2.21)], and hence positron emission towards counter 3 is increased. This increase in positron counts in counters 3 and 4 due to the microwave power is the signal of an induced transition and it is given in Eq. (2.28). The signal is measured as a function of magnetic field H, with fixed microwave frequency and power.

B. Magnet

The magnet was the solenoidal type magnet consisting of a set of two thick coils surrounded by an iron sheath, which has been described in Ref. 2. A 300-kW motor-generator set supplied the exciting current of 600 A, and its output voltage was regulated to 0.1%.

The magnetic field H used was 5800 G, which was close to the maximum field achievable. The average magnetic field over the volume of the microwave cavity, which was 24.2 cm in length and 19.48 cm in diameter and was placed at the center of the magnet, was 12 G higher than the central field. The standard deviation of H over this volume was 15 G, which is a fractional homogeneity of 0.25%.

The magnetic field was calibrated and monitored to an accuracy of 0.05% with an NMR probe using H_2O with 0.1 N LiCl. During the data taking, the field was monitored at a point just outside the gas target where the field differed from the central field by 11 G.

C. Gas Target

The gas target shown in Fig. 4 consisted of a cylindrical pressure vessel made of 304 stainless steel inside of which an aluminum microwave cavity was mounted. The front window of the pressure vessel through which the muons enter had a thickness of 0.178 cm. Three ports were placed in the midsection; one was used for a microwave power input connector and the other two for gas inlet and outlet ports.

The target was filled with argon at a pressure of 800 lb/in.^{2}. The gas handling and gas purification systems were the same as described in Ref. 2, and the heated titanium sponge[62] over which the argon was continuously recirculated was operated at a temperature of 750 °C, where the gettering rate was high. This temperature was chosen on the basis of studies of the gettering rate of air by the titanium as a function of its temperature. Mass spectroscopic analyses indicated that these procedures resulted in argon gas in the target with impurities of other than noble gases of less than 10 ppm.

D. Microwave System

The requirement on the microwave system was to provide a magnetic field $\vec{H}_1 \cos\omega t$ of the proper frequency, amplitude, and polarization to induce the transition between muonium states 1 and 2. At the static magnetic field H of 5800 G, the resonant frequency ν_{12} is approximately 1850 MHz, as given by Eqs. (2.14) and in Fig. 2. The required amplitude H_1 can be determined from Eq. (2.21) and Table I. The transition probability will be maximum ($|a_2|^2 = 1/e$) for $t = 1/\gamma$ if $H_1 = 1.3$ G. Since this initial experiment had as its goal the

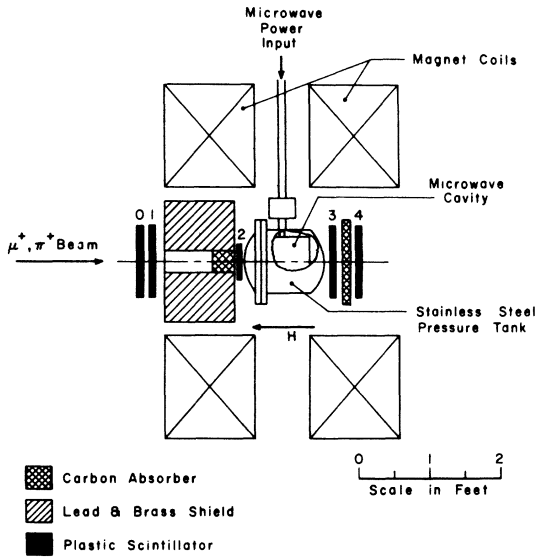

FIG. 3. Schematic diagram of the experimental arrangement, indicating the high-pressure gas target containing the microwave cavity, the scintillation detectors (numbered 0–4), and the magnet. Scintillation counters 0, 1, and 4 were 8-in.-diam circular counters and counters 2 and 3 were square counters 3 in. ×3 in. × $\frac{1}{8}$ in. and 10 in. ×10 in. × $\frac{1}{2}$ in., respectively.

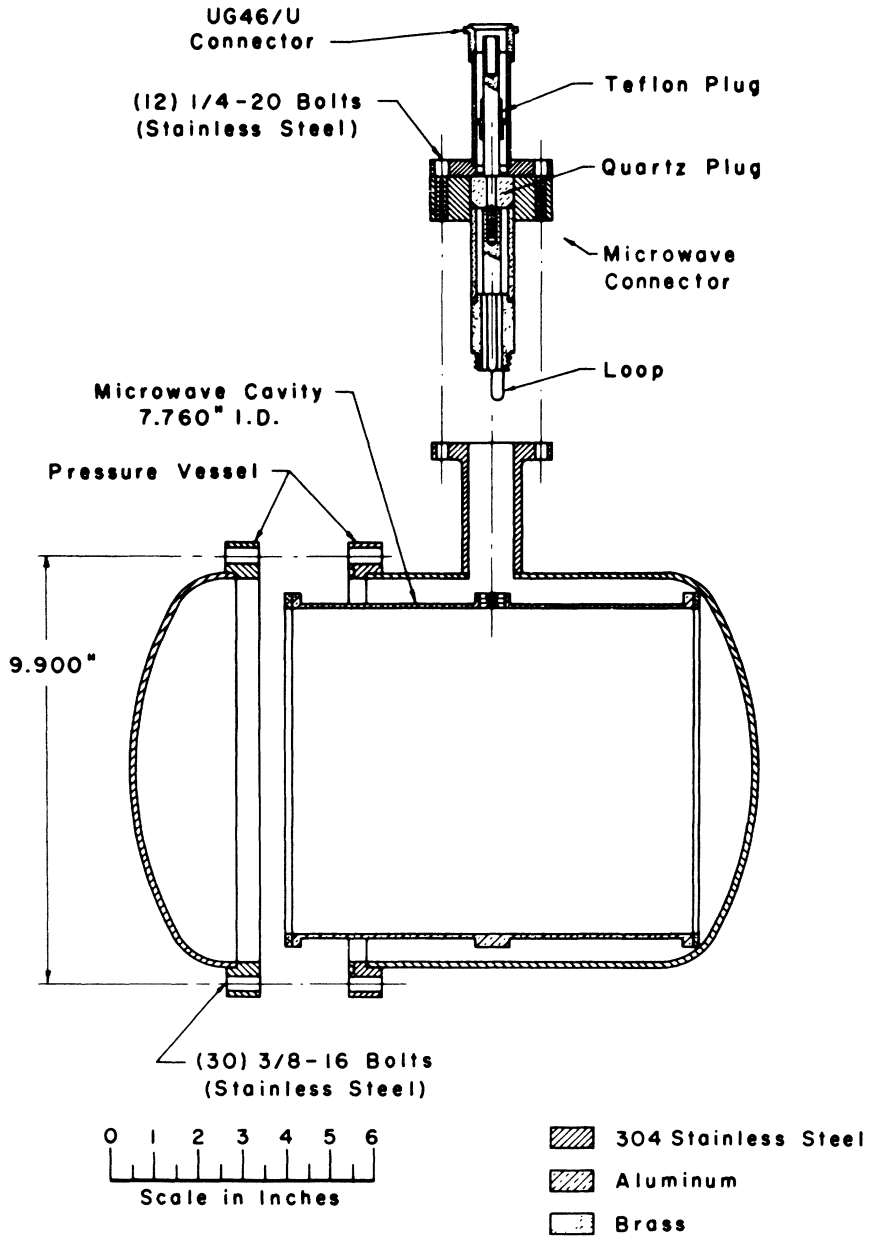

FIG. 4. Cross-section view of the gas target vessel containing the microwave cavity.

first observation of an induced resonance transition in muonium, it was decided to use a higher microwave field ($H_1 \simeq 8.5$ G was attainable with our microwave system) which would yield a very broad resonance line which would be easy to observe. The direction of $\vec{H}_1$ must be perpendicular to $\vec{H} = H\hat{k}$ in order to induce the transition $1 \leftrightarrow 2$ for which $\Delta M = \pm 1$.

A block diagram of the microwave system is shown in Fig. 5. The microwave cavity operated in the TM_{110} mode, which had the following favorable characteristics: (a) A cavity resonant frequency of 1850 MHz is obtained with a convenient diameter of 19.48 cm for the cylindrical cavity. (b) The field $\vec{H}_1$ in the cavity does not depend on the axial coordinate z and has no z component. Furthermore it has a simple dependence on the cylindrical coordinates r and θ. (c) The TM_{110} mode is a low-order mode and is well separated from other modes. The cavity was 24.2 cm in length and its unloaded Q was about 26 000. The temperature dependence of its resonant frequency was approximately 20 ppm/°C. The microwave power was fed into the cavity through a high-pressure microwave connector which was terminated with a loop of about 0.8-cm^2 area. The size and orientation of the loop were adjusted to give a voltage standing-wave ratio (VSWR) of less than 1.1.

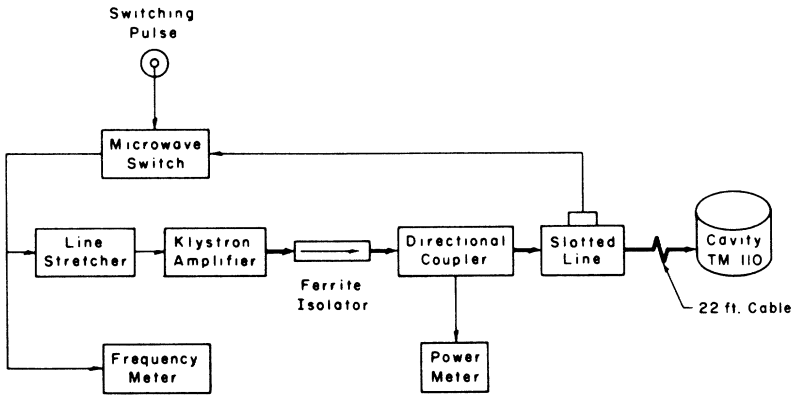

FIG. 5. Block diagram of the microwave cavity.

The source of microwave power was a 1-kW cw klystron amplifier (Varian C model No. 802B) as part of an oscillator circuit including the microwave cavity. The resonant frequency of the cavity determined the oscillation frequency. The feedback signal was obtained from a microwave pickup probe in the slotted line and was fed to the input of the klystron amplifier through a line stretcher which provided phase adjustment. The oscillator frequency drifts due to thermal changes of the cavity were negligible for the accuracy of the initial experiment reported in this paper. The microwave frequency was measured to an accuracy of about 10 ppm by coupling out a small signal from the feedback loop and using a transfer oscillator[63] and a superheterodyne frequency counter.[64] The short-term stability of the oscillator was better than 10 ppm.

The amplitude of the microwave magnetic field at the center of the cavity was 8.5 G when the full 1-kW output from the klystron amplifier was used. This field produced a resonance linewidth about 30 times the natural width of 4 G, or 120 G as the full width at half-maximum (FWHM), when the resonance line is obtained with fixed microwave frequency by varying the static magnetic field [see Eq. (2.28) and Table I]. The microwave power level was monitored with a 30-dB directional coupler and a bolometer.[65]

Using the microwave switch[66] in the feedback line, the microwave power was pulsed on and off in alternate beam cycles as discussed in Sec. III E. In order to reduce heating of the microwave cavity, the power was pulsed on only during the time the synchrocyclotron beam struck the internal target.

E. Particle Detectors and Electronics

The particle detectors indicated in Fig. 3 were scintillation counters, each viewed by a magnetically shielded 6810A photomultiplier tube through a 2-ft light pipe. The electronic logic system is indicated by a block diagram in Fig. 6. The component circuits were similar to those described in Ref. 2. A muon stopped in the target was indicated by a $12\bar{3}$ coincidence and a decay positron by a $34\bar{2}$ coincidence. The stopped muon pulse ($12\bar{3}$) opened a 3.2-μsec gate after a 0.1-μsec delay, the gate being formed by a shorted delay line and a Schmitt trigger circuit. A positron pulse ($34\bar{2}$) occurring during the gate was registered as an event. Event pulses and ungated $34\bar{2}$ pulses were switched alternately to two sets of scalers in synchronism with the microwave on-off switching pulses. Accidental counts were monitored by requiring a coincidence between the gate and a $34\bar{2}$ pulse delayed by 3.3 μsec. Typical counting rates relative to the $12\bar{3}$ rate were as follows: ungated $34\bar{2}$, 6%; events, 3%; and accidentals, 0.1%.

The microwave power was switched on and off during alternate beam cycles, each beam cycle consisting of four bursts separated by 1/60 sec. This procedure assured that the muon beam at the target was the same with the microwaves on and off, since the frequency modulation of the synchrocyclotron was obtained with a set of rotating condensers with four blades. The microwave switching pulses were derived from the cyclotron marker pulses.

IV. DATA AND DATA ANALYSIS

A. Experimental Procedure

The muon beam was similar to that described in Ref. 2. For the present experiment the beam momentum was 140 MeV/c, and a magnetic channel provided magnetic shielding.[67] A muon-beam duty cycle of 2% was used (although a much longer duty cycle was available with a vibrating target[68]) because of the high instantaneous microwave power required. With the pressure vessel filled with argon to a pressure of 50 atm, the target stopping power was 6.2 g/cm^2, and approximately 450 stopped muons per second were obtained.

Pure argon gas at pressures between 35 and 50 atm was used in the target. The gas purifier was operated for 2 days before data were taken, and the purifier was operated continuously throughout

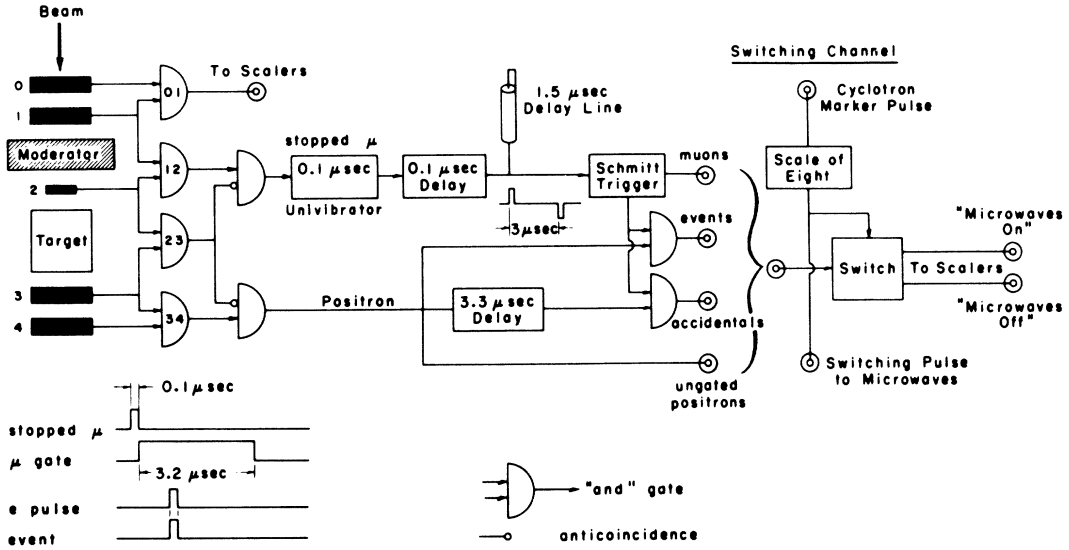

FIG. 6. Block diagram of electronic logic system.

the data taking.

Data for a particular resonance curve were taken as a function of the static magnetic field with fixed microwave frequency and power. For each point on a resonance curve, data were taken for about 40 min which corresponded to about 10^6 stopped muons. Values for the gas pressure, magnetic field, microwave frequency, and microwave power were recorded, in addition to the $12\bar{3}$, ungated $34\bar{2}$, event and accidental counts for the conditions of microwaves on and off. Data were obtained for three resonance curves for three different conditions of argon pressure and microwave power as indicated in Table II. For each curve, between 40 and 70 points were taken. About 200 h of data taking were obtained.

B. Data Analysis

The data for each curve were fit to a Lorentzian line shape. For each data point the observed signal height y was computed as follows:

$$y=\frac{(E'/N'-A'/N')-(E/N-A/N)}{(E/N-A/N)}, \qquad (4.1)$$

in which N, E, and A are the number of stopped muons ($12\bar{3}$), events and accidental counts with the microwave power off, respectively, and the primed symbols are the same quantities with the microwave power on. Then the set of points for magnetic field and signal, (H_α, y_α), were fit by a least-squares procedure to the simple Lorentzian line shape:

$$S_\alpha = A_0/[\Delta^2+(H_\alpha-H_0)^2]. \qquad (4.2)$$

The amplitude A_0, the linewidth Δ, and the center or resonance field H_0 are all parameters to be determined from the fit, and the quantities S_α and H_α are the signal and corresponding magnetic field.

The justification for the representation of the data by Eq. (4.2) is provided by Eq. (2.28). In Eq. (4.2) the resonance term in the denominator is $(H_\alpha-H_0)^2$ rather than $(\omega-\omega_{12})^2$ as in Eq. (2.28). This substitution is an approximation as can be seen from Eqs. (2.14), and it is adequate for the accuracy of the present paper since the linewidth in magnetic field ΔH (FWHM) is a small fraction of the center field H_0. The theoretical line shape given in Eq. (4.2) neglects the following factors: (a) variation of the static magnetic field over the microwave cavity volume; (b) variation of the amplitude of the microwave magnetic field over the cavity volume; (c) variation of effective solid

TABLE II. Data and results of analysis for observed resonance lines.

Line designation	Number of data points	Argon	Microwave power (W)	Microwave frequency (MHz)	Line center, H_0 (G)	Linewidth (FWHM) (G)	$\Delta\nu$ (MHz)
1	64	50	800	1850.083	5725	120	4461.21
2	70	50	240	1850.673	5742	44	4461.09
3	42	35	400	1859.595	5988	66	4461.78

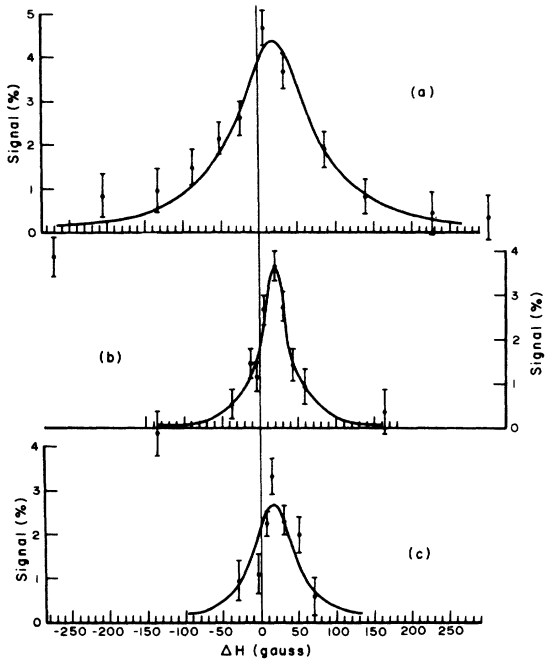

FIG. 7. Observed signal height as a function of static magnetic field. The three curves were taken under the following conditions of argon gas pressure and microwave input power: (a) 50 atm, 800 W; (b) 50 atm, 240 W; (c) 35 atm, 400 W. The zero of the horizontal axis is the expected line center, which is calculated under the assumption that there is no hfs pressure shift. The solid lines are least-squares fit Lorentzian functions calculated as described in the text.

angle for positron detection over the cavity volume; (d) effect of static magnetic field on decay positron trajectories, and hence on positron detection efficiency, as a function of momentum and position of origin in the cavity; (e) distribution of stopping muons in the cavity; and (f) finite gate time for observation of decay positrons. The neglect of all of these effects constitutes approximations which are valid for the purposes of the present paper; the third paper of this series will treat these effects.

A least-squares fit of the data points for each resonance curve to the Lorentzian function Eq. (4.2) was made and the χ^2 value was computed:

$$\chi^2 = \sum_{\alpha=1}^{n} \frac{(y_\alpha - S_\alpha)^2}{\sigma_\alpha^2} \quad , \tag{4.3}$$

in which σ_α is the standard deviation of y_α calculated from the statistical counting error. The parameters A, Δ^2, and H_0 were chosen to minimize χ^2.

Table II gives data on the fits for the three resonance curves. The χ^2 values indicated satisfactory fits. In order to obtain the field value H_0, the weighted average field over the cavity, considering the solid angle factor subtended by the positron detector at each point, was calculated.

The resonance curves are shown in Fig. 7. For purposes of display, the many experimental points are grouped together and statistical counting errors are indicated. The solid curves are the fits to the data given in Table II. The first resonance curve [Fig. 7(a)] observed was that with an argon pressure of 50 atm and a peak microwave input power of 800 W. The FWHM value of the line is about 120 G. The natural linewidth given by Eqs. (2.17) and (2.30) is only 4 G and the static magnetic field inhomogeneity is about 15 G; the principal cause of the linewidth is microwave power broadening. The maximum signal intensity is 4% and can be estimated as follows:

$$S_{max} = f_1 f_2 f_3 f_4 f_5 f_6 = (0.8)(0.8)(0.4)(0.5)(0.5)(0.8)$$
$$= 0.05 \quad , \tag{4.4}$$

where f_1 is the fraction of muons in stopping beam, $\simeq 0.8$; f_2 is the polarization of muon beam, $\simeq 0.8$; f_3 is the fraction of muons stopping in gas and forming muonium in cavity, $\simeq 0.4$; f_4 is the fraction of muonium atoms in state 1, $\simeq 0.5$; f_5 is the fractional change in decay positron detection probability associated with microwave induced transition causing a saturation mixing of states 1 and 2, $\simeq 0.5$; and f_6 is the factor associated with finite solid angle subtended by positron detector at gas target, which reduces effective asymmetry of positron decay from different muon spin states, $\simeq 0.8$. The theoretical estimate of S_{max} is in good agreement with the observed maximum signal of 4%.

The second resonance curve [Fig. 7(b)] was taken with a reduced microwave power of 240 W, and its FWHM value is 40 G. The third resonance curve [Fig. 7(c)] was taken with a lower gas pressure of 35 atm, and has a somewhat lower signal due to the smaller fraction of the muons stopping in the gas relative to the walls and counter 2.

C. Effect of Gas Impurities and Microwave Electric Field: Muonium Chemistry

After the data shown in Table II were obtained, a brief study was made of the effect of gas impurities in the argon on the intensity of the resonance signal.[69] The procedure was to add small amounts of air to argon at a pressure of 50 atm and then to observe the maximum intensity of the resonance signal. Addition of xenon to the argon was also studied. The results are shown in Table III. It is clear that air as an impurity reduces the resonance signal, and, in sufficient amount, eliminates the signal entirely. The xenon, even in relatively large amount, produced no effect on the resonance signal. These data constituted our first

TABLE III. Effect of gas impurities on resonance signal.

Target gas	Signal intensity (%)
Tank argon (Linde)	6.10 ± 0.60
90% tank argon + 10% xenon	6.37 ± 0.60
Tank argon + 70-ppm air	2.12 ± 0.60
Tank argon + 200-ppm air	0.35 ± 0.69

observations of muonium chemistry which was later studied in some detail.[70] The effect of air in reducing the signal is believed to be due principally to depolarization of muonium in spin exchange collisions with oxygen. Xenon is not expected to have an effect on the signal because muonium formation in xenon should have a near unity probability as it does for muons stopped in argon, and muonium collisions with xenon should not depolarize muonium. It is worth noting that a good resonance signal was observed with tank argon without further purification. It is plausible that the present high-field resonance experiment is less sensitive to gas impurity than the low-field muonium precession experiment.[2]

For positronium, an electric field increases the fraction of the positrons stopped in a gas that form positronium, due to the acceleration of slow positrons.[71] In order to determine whether or not such an effect is important for muonium, the signal y of Eq. (4.1) was measured at an argon pressure of 50 atm and at the maximum microwave power, using an off-resonance static magnetic field value of $H = 100$ G. The signal y associated with the microwave field was zero to within the statistical error of 0.01, thus indicating that the microwave electric field does not appreciably increase the formation of polarized muonium. In view of the theory[2] that muonium is formed at energies well above the threshold energy and also of the smallness of the parameter E/p (E is the amplitude of microwave electric field and p is the argon gas pressure), which characterizes the gain in energy of the muon from the electric field, this observed result was to be expected.

V. RESULTS AND CONCLUSIONS

Values for the hfs interval $\Delta\nu$ were obtained from the observed values of the microwave frequency $\nu = \nu_{12}$ and corresponding center magnetic field value H_0, as given in Table II. An equation for $\Delta\nu$ is obtained by solving Eqs. (2.14),

$$\Delta\nu = \frac{[\nu_{12} - (\mu_B^{\mu} g'_{\mu}/\mu_B^{e} g'_{p})H_0]\,[\nu_{12} - (g_J/g'_{p})H_0]}{\nu_{12} - [(g_J/g'_{p}) + (\mu_B^{\mu} g'_{\mu}/\mu_B^{e} g'_{p})]H_0/2}\,, \quad (5.1)$$

in which g'_p is the g value of protons in water defined in terms of the electron Bohr magneton μ_B^e, and the static magnetic field H_0 is expressed as the proton resonance frequency in water. We use the measured values[30,72]

$$\frac{\mu_B^{\mu} g'_{\mu}}{\mu_B^{e} g'_{p}} = 3.183\,363 \pm 0.000\,041 \text{ (13 ppm)}, \quad (5.2)$$

$$\frac{g_J}{g'_{p}} = -658.215\,909 \pm 0.000\,044 \text{ (0.07 ppm)}. \quad (5.3)$$

The value for $\mu_B^{\mu} g'_{\mu}/\mu_B^{e} g'_{p}$ is obtained from Eqs. (2.6) and (2.13), together with a measured value[73] of 26.0×10^{-6} for the magnetic shielding of protons in water. Hence, using Eq. (5.1), we obtain the values of $\Delta\nu$ given in Table II.

The error in each $\Delta\nu$ value is due principally to the inhomogeneity of the static magnetic field. The rms standard deviation $(\Delta H)_{\text{rms}}$ of H over the cavity volume was 14.1 G, as discussed in Sec. III B. (This standard deviation was weighted by the solid angle subtended by the positron detector.) Using the expression for $\partial\nu_{12}/\partial H$ of Eqs. (2.17) and (5.1), we obtain the error contribution due to magnetic field inhomogeneity as

$$\frac{\partial\Delta\nu}{\partial H}\Big|_{H=H_0} (\Delta H)_{\text{rms}} = 1.4 \text{ MHz}. \quad (5.4)$$

The second important error source is the hfs pressure shift. Since the experiment reported in this paper was not sufficiently accurate to detect a pressure shift, the value of the linear fractional pressure shift for hydrogen in argon measured in optical pumping experiments at relatively low pressure[74] is taken to represent the fractional pressure shift for muonium in argon. Hence using

$$\frac{1}{\Delta\nu}\frac{\partial\Delta\nu}{\partial p} = -(4.78 \pm 0.03) \times 10^{-9}/\text{Torr at } 0\,^{\circ}\text{C}, \quad (5.5)$$

we find a shift of -0.81 MHz at 50 atm, which is considered as an error.

The combined error from the two above sources is obtained by adding the errors in quadrature to give 1.6 MHz. The statistical counting error is relatively small, and we take the over-all error estimate to be 2.0 MHz.

The final result for $\Delta\nu$ is obtained by averaging the three values given in Table II, weighted by the number of individual data points for each resonance curve. The value is

$$\Delta\nu_{\text{expt}} = 4461.3 \pm 2.0 \text{ MHz}, \quad (5.6)$$

in which the error is a 1 standard deviation error.

This experimental result agrees with the theoretical value

$$\Delta\nu_{\text{theor}} = 4463.282 \pm 0.062 \text{ MHz (14 ppm)} \quad (5.7)$$

given in Eq. (2.10) to within the experimental error of 1 part in 2200. This agreement provides a confirmation of the theoretical formula for $\Delta\nu$ [Eq. (2.1)] to the term of order $\alpha^3 R_\infty$.

A precision measurement of $\Delta\nu$ by the method of this paper will be described in the third paper of this series.

*Research supported in part by the U. S. Air Force (OSR) (with Yale University) and by the National Science Foundation (with Columbia University).

†Present address: CERN, Geneva, Switzerland.

‡Present address: Physics Department, University of Pittsburgh, Pittsburgh, Pa. 15213.

§Present address: Physics Department, University of Wisconsin, Madison, Wisc. 53706

‖Present address: Physics Department, University of Virginia, Charlottesville, Va. 22903.

[1]V. W. Hughes, D. W. McColm, K. Ziock, and R. Prepost, Phys. Rev. Letters 5, 63 (1960).

[2]V. W. Hughes, D. W. McColm, K. Ziock, and R. Prepost, Phys. Rev. A 1, 595 (1970); Phys. Rev. A 2, 551 (1970).

[3]R. Prepost, V. W. Hughes, and K. Ziock, Phys. Rev. Letters 6, 19 (1961).

[4]G. Kallén, in *Encyclopedia of Physics*, edited by S. Flügge (Springer, Berlin, 1958), Vol. V/1, p. 169.

[5]G. Feinberg and L. M. Lederman, Ann. Rev. Nucl. Sci. 13, 431 (1963).

[6]K. Ziock, V. W. Hughes, R. Prepost, J. Bailey, and W. Cleland, Phys. Rev. Letters 8, 103 (1962); J. Bailey, W. Cleland, V. W. Hughes, R. Prepost, and K. Ziock, in *International Conference on High-Energy Physics*, edited by J. Prentki (CERN, Geneva, 1962), p. 473.

[7]V. W. Hughes, Ann. Rev. Nucl. Sci. 16, 445 (1966).

[8]W. E. Cleland, J. M. Bailey, M. Eckhause, V. W. Hughes, R. M. Mobley, R. Prepost, and J. E. Rothberg, Phys. Rev. Letters 13, 202 (1964).

[9]R. D. Ehrlich, H. Hofer, A. Magnon, D. Stowell, R. A. Swanson, and V. L. Telegdi, Phys. Rev. Letters 23, 513 (1969).

[10]P. A. Thompson, J. J. Amato, P. Crane, V. W. Hughes, R. M. Mobley, G. zu Putlitz, and J. E. Rothberg, Phys. Rev. Letters 22, 163 (1969).

[11] P. Crane, J. J. Amato, V. W. Hughes, D. M. Lazarus, G. zu Putlitz, and P. A. Thompson, in *High-Energy Physics and Nuclear Structure*, edited by S. Devons (Plenum, New York, 1970), p. 677.

[12]H. A. Bethe and E. E. Salpeter, in *Encyclopedia of Physics*, edited by S. Flügge (Springer, Berlin, 1957), Vol. 35/1, p. 88

[13]S. J. Brodsky and G. W. Erickson, Phys. Rev. 148, 26 (1966).

[14]E. Fermi, Z. Physik 60, 320 (1930).

[15]G. Breit and R. E. Meyerott, Phys. Rev. 72, 1023 (1947).

[16]G. Breit, Phys. Rev. 35, 1447 (1930).

[17]C. M. Sommerfield, Ann. Phys. (N. Y.) 5, 26 (1958).

[18]A. Petermann, Fortschr. Physik 6, 505 (1958).

[19]S. D. Drell and H. R. Pagels, Phys. Rev. 140, B397 (1965).

[20]R. G. Parsons, Phys. Rev. 168, 1562 (1968).

[21]J. A. Mignaco and E. Remiddi, Nuovo Cimento 60A, 519 (1969).

[22]J. Aldins, T. Kinoshita, S. J. Brodsky, and A. J. Dufner, Phys. Rev. Letters 23, 441 (1969).

[23]R. Karplus and A. Klein, Phys. Rev. 85, 972 (1952).

[24]N. M. Kroll and F. Pollack, Phys. Rev. 86, 876 (1952).

[25]A. Layzer, Nuovo Cimento 33, 1538 (1964).

[26]D. E. Zwanziger, Nuovo Cimento 34, 77 (1964).

[27]R. Arnowitt, Phys. Rev. 92, 1002 (1953).

[28]W. A. Newcomb and E. E. Salpeter, Phys. Rev. 97, 1146 (1955).

[29]D. P. Hutchinson, J. Menes, G. Shapiro, and A. M. Patlach, Phys. Rev. 131, 1351 (1963).

[30]D. P. Hutchinson, F. L. Larsen, N. C. Schoen, D. I. Sober, and A. S. Kanofsky, Phys. Rev. Letters 24, 1254 (1970). In Eq. (2.4) we use the quoted value of the more recent Ref. 30, which is in agreement with the less precise value of the older Ref. 29.

[31]M. A. Ruderman, Phys. Rev. Letters 17, 794 (1966).

[32]B. N. Taylor, W. H. Parker, and D. N. Langenberg, Rev. Mod. Phys. 41, 375 (1969).

[33]T. Myint, D. Kleppner, N. F. Ramsey, and H. G. Robinson, Phys. Rev. Letters 17, 405 (1966).

[34]W. H. Parker, B. N. Taylor, and D. N. Langenberg, Phys. Rev. Letters 18, 287 (1967).

[35]W. H. Parker, D. N. Langenberg, A. Denenstein, and B. N. Taylor, Phys. Rev. 177, 639 (1969).

[36]T. F. Finnegan, A. Denenstein, and D. N. Langenberg, Phys. Rev. Letters 24, 738 (1970).

[37]J. Bailey, W. Bartl, G. Von Bochmann, R. C. A. Brown, F. J. M. Farley, H. Jostlein, E. Picasso, and R. W. Williams, Phys. Letters 28B, 287 (1968).

[38]J. C. Wesley and A. Rich, Phys. Rev. Letters 24, 1320 (1970).

[39]R. Gatto, in *High Energy Physics*, edited by E. H. S. Burhop (Academic, New York, 1967), Vol. II, p. 1.

[40]E. Picasso, in *High-Energy Physics and Nuclear Structure*, edited by S. Devons (Plenum, New York, 1970), p. 615.

[41]J. Bailey and E. Picasso, Progr. Nucl. Phys. 12, 43 (1970).

[42]T. D. Lee and G. C. Wick, Nucl. Phys. B9, 209 (1969).

[43]S. D. Drell, in *Atomic Physics*, edited by V. W. Hughes, B. Bederson, V. W. Cohen, and F. M. J. Pichanick (Plenum, New York, 1969), p. 53.

[44]N. M. Kroll, Nuovo Cimento 45A, 65 (1966).

[45]N. M. Kroll, in *Physics of the One-and Two-Electron Atoms*, edited by F. Bopp and H. Kleinpoppen (North-Holland, Amsterdam, 1969), p. 179.

[46]S. J. Brodsky, in *Proceedings of the Fourth International Symposium on Electron and Photon Interactions at High Energies*, 1969, edited by D. W. Braden (McCorquodale, Ltd., Lancashire, England, 1969), p. 15.

[47]V. W. Hughes, in *Atomic Physics*, edited by V. W. Hughes, B. Bederson, V. W. Cohen, and F. M. J. Pichanick (Plenum, New York, 1969), p. 15.

[48]D. R. Yennie, in *Proceedings of* 1967 *International Conference on Electron and Photon Interactions at High Energies* (U. S. Dept. of Commerce, Springfield, Va., 1967), p. 32.

[49]G. Feinberg, in *International Conference on High-Energy Physics*, edited by J. Prentki (CERN, Geneva, 1962), p. 879; D. L. Morgan, Jr., Ph.D. thesis, Yale University 1966 (unpublished).

[50]S. J. Brodsky and J. R. Primack, Ann. Phys. (N.Y.) 52, 315 (1969).

[51]P. Kusch and V. W. Hughes, in *Encyclopedia of Physics*, edited by S. Flügge (Springer, Berlin, 1959), Vol. 37/1, p. 1.

[52]G. Breit, Nature 122, 649 (1928).

[53]W. E. Lamb, Jr., Phys. Rev. 60, 817 (1941).

[54]F. Bloch and A. Siegert, Phys. Rev. 57, 522 (1940).

[55]N. Barash-Schmidt, A. Barbaro-Galtieri, L. R. Price, A. H. Rosenfeld, P. Söding, C. G. Wohl, M. Roos, and G. Conforto, Rev. Mod. Phys. 41, 109 (1969).

[56]V. F. Weisskopf and E. P. Wigner, Z. Physik 63, 54 (1930); 65, 18 (1930).
[57]W. E. Lamb, Jr., Phys. Rev. 85, 259 (1952).
[58]F. E. Low, Phys. Rev. 88, 53 (1952).
[59]G. Kallén, *Elementary Particle Physics* (Addison-Wesley, London, 1964), p. 375.
[60]T. D. Lee and C. S. Wu, Ann. Rev. Nucl. Sci. 15, 381 (1965).
[61]W. E. Cleland, Ph.D. thesis, Yale University, 1964 (unpublished). Additional details on the experiment are given in this thesis.
[62]The titanium sponge was Grade A1 obtained from E. I. du Pont de Nemours and Co.
[63]Hewlett-Packard model No. 540 B.
[64]Beckman model No. 7370 output meter and Model No. 7570 counter series.
[65]Hewlett-Packard model No. 430 C.
[66]Microwave Associates model No. MA 3459.
[67]M. Bardon, P. Franzini, and J. Lee, Phys. Rev. 126, 1826 (1962).
[68]J. Rosen, Nevis Report No. 92, Columbia University (unpublished).
[69]J. Bailey, W. Cleland, V. W. Hughes, R. Prepost, and K. Ziock, Bull. Am. Phys. Soc. 7, 264 (1962).
[70]R. M. Mobley, J. M. Bailey, W. E. Cleland, V. W. Hughes, and J. E. Rothberg, J. Chem. Phys. 44, 4354 (1966); R. M. Mobley, J. J. Amato, V. W. Hughes, J. E. Rothberg, and P. A. Thompson, *ibid.* 47, 3074 (1967); R. M. Mobley, J. M. Bailey, W. E. Cleland, V. W. Hughes, and J. E. Rothberg, in *Fourth International Conference on the Physics of Electronic and Atomic Collisions, Quebec*, 1965 (Science Bookcrafters, Hasting-on-Hudson, N. Y., 1965), p. 194.
[71]S. Marder, V. W. Hughes, C. S. Wu, and W. R. Bennett, Jr., Phys. Rev. 103, 1258 (1956); W. B. Teutsch and V. W. Hughes, *ibid.* 103, 1266 (1956).
[72]E. B. D. Lambe, *Polarization, Matière, et Rayonnement* (Societé Francaise de Physique, Paris, 1969), p. 441.
[73]N. F. Ramsey, *Nuclear Moments* (Wiley, New York, 1953).
[74]R. A. Brown and F. M. Pipkin Phys. Rev. 174, 48 (1968); F. M. Pipkin and R. H. Lambert, *ibid.* 127, 787 (1962).

PHYSICAL REVIEW A VOLUME 3, NUMBER 3 MARCH 1971

Fine-Structure Measurement of Singly Ionized Helium, $n = 4$*

Ralph R. Jacobs,† Kenneth R. Lea, and Willis E. Lamb, Jr.
Yale University, New Haven, Connecticut 06520
(Received 15 June 1970)

Precision measurements of the energy differences $\delta_4(4\,^2S_{1/2}-4^2P_{1/2})$ and $\Delta E_4-\delta_4(4\,^2P_{3/2}-4\,^2S_{1/2})$ in $(He^4)^+$ are reported. The experimental results, $\delta_4=1768\pm5$ MHz and $\Delta E_4-\delta_4=20\,179.7\pm1.2$ MHz, agree with the values predicted by quantum electrodynamic theory, $\delta_4=1768.34\pm0.51$ MHz and $\Delta E_4-\delta_4=20\,180.78\pm0.56$ MHz. An electron gun excites the states of interest in a section of waveguide containing helium gas. A magnetic field applied perpendicular to the waveguide axis is used to scan a microwave resonance between suitable Zeeman levels for a fixed frequency of oscillating electric field in the waveguide. Any induced electric dipole transitions $4\,^2S_{1/2}\rightarrow 4\,^2P_{1/2}$ or $4\,^2S_{1/2}\rightarrow 4\,^2P_{3/2}$ reduce the intensity of 1215-Å radiation which is emitted in the natural decay of $4S$ to $2P$. This light is directed onto an ultraviolet-detecting phototube whose output is measured by a lock-in detector for which the synchronous signal is provided by square-wave amplitude modulation of the microwave field. The resonances obtained by varying the magnetic field are fitted to a theoretical line-shape formula by a computerized least-squares program. The resulting best-fit parameters include either δ_4 or $\Delta E_4-\delta_4$, depending on the transition studied. Consideration is given to the dependence of the resonance center on the gun current, helium pressure, and microwave power level.

I. BASIS OF THE EXPERIMENT

A. Introduction

The fine structure of one-electron atoms has been the subject for much experimental and theoretical investigation since 1947, when Lamb and Retherford[1] discovered that, contrary to the Dirac theory, the states $2\,^2S_{1/2}$ and $2\,^2P_{1/2}$ in hydrogen were nondegenerate. In addition to the "Lamb shift" δ_n (interval between $n\,^2S_{1/2}$ and $n\,^2P_{1/2}$), another important energy separation $\Delta E_n=n\,^2P_{3/2}-n\,^2P_{1/2}$ can be determined, which yields a value for the fine-structure constant α, the expansion parameter in quantum-electrodynamic (QED) theory.[2,3] In the case of hydrogen, disagreements have existed among different experiments and between experiment and theory on the value of δ_2 as well as among various experimental results for the value of ΔE_2. The present research was undertaken with the ultimate hope that fine-structure measurements in the $n=4$ term of singly ionized helium would remove some of the difficulties surrounding the value of δ_2 in H by limiting the coefficients of certain uncalculated n- and Z-dependent QED terms, and perhaps, through the value of ΔE_4, provide another competitive determination of α. This paper reports the